# Tectonic geodesy revealing geodynamic complexity of the Indo-Burmese arc region, North East India

## Bhaskar Kundu and V. K. Gahalaut*

CSIR-National Geophysical Research Institute, Uppal Road, Hyderabad 500 007, India

The plate boundary between India and Sunda plates across the Indo-Burmese arc (IBA) region is probably the most neglected domain as far as the plate motion, crustal deformation and earthquake occurrence processes are concerned. Because of the limited or no geodetic measurements across the IBA region, debate continues on the most appropriate plate boundary model for the region. Subduction along this boundary occurred in geological past, but whether it is still active is a debatable issue. It is believed that the predominantly northward India–Sunda relative plate motion of about 36 mm/year is partitioned between the Indo-Burmese wedge (IBW) and the Sagaing Fault (SF). However, it is not clear how relative plate motion between India and Sunda plates is accommodated across the IBA region – whether localized, partitioned or distributed, and in particular what is the slip rate and mode of slip accommodation across faults in the region? In such cases, Global Positioning System (GPS) measurements of crustal deformation have proved to be the best and probably the only tool. Our detailed seismo-tectonic study, crustal deformation study using high precision GPS measurements of eight years, strain rate estimates, field studies, analytical and finite element modelling of GPS data from the IBW region in North East India provide evidence for present-day active deformation front (or the plate boundary fault) between the India and Burma plates. On the basis of our extensive studies, it is now suggested that the Churachandpur–Mao Fault (CMF), a geologically older thrust fault, accommodates motion of about 16 mm/year through dextral strike–slip manner. The motion across the CMF constitutes about 43% of the relative plate motion of 36 mm/year between the India and Sunda plates. The remaining motion is accommodated at SF. On the basis of modelling, which suggests low friction along the CMF, absence of low-magnitude seismicity along the CMF, lack of historic and great and major earthquakes on the CMF and regions around it, and field studies, it is proposed that the motion across the CMF occurs predominantly in an aseismic manner. Such behaviour of the CMF significantly lowers the seismic hazard in the region.

**Keywords:** Churachandpur–Mao Fault, Global Positioning System, Indo-Burmese arc, subduction.

## Introduction

'Geology began when early man first picked up a stone, considered its qualities, and decided that it was better than the stone he already had…'.

–Faul and Faul[1]

FROM the beginning of the journey of geoscience, with the discovery of new data resources and advanced methodologies, we have refined our understanding regarding the geodynamic complexity of seismo-tectonically active regions. Specially, in the field of 'tectonic geodesy' (a discipline dealing with the application of geodetic techniques in understanding tectonic processes), space-based geodetic techniques [e.g. Global Positioning System (GPS), Very Long Baseline Interferometry (VLBI), Inter-ferometric Synthetic Aperture Radar (InSAR), Doppler Orbitography and Radiopositioning Integrated by Satellite (DORIS), Satellite Laser Ranging (SLR), etc.] now provide quantitative maps of the surface velocity field within tectonically active regions, supplying constraints on the spatial distribution of the lithospheric deformation process. GPS measurement for crustal deformation is a cheaper, impressive, precise and portable geodetic tool with many advantages over other space-based geodetic techniques. In studies related to geodynamics, GPS measurements provide estimates of plate motion at a site, various phases of deformation through earthquake cycle, evidence of strain accumulation, deformation caused by anthropogenic activities, etc.[2–7]. All these aspects are important in quantitative and objective assessment of seismic hazard of a region. Amongst all techniques only tectonic geodesy provides information on the above aspects and this is what makes it indispensable in earthquake-related studies.

In this review article, we demonstrate the capability of this technique in solving a long-standing problem of relative plate motion and its rate and mode of accommodation in
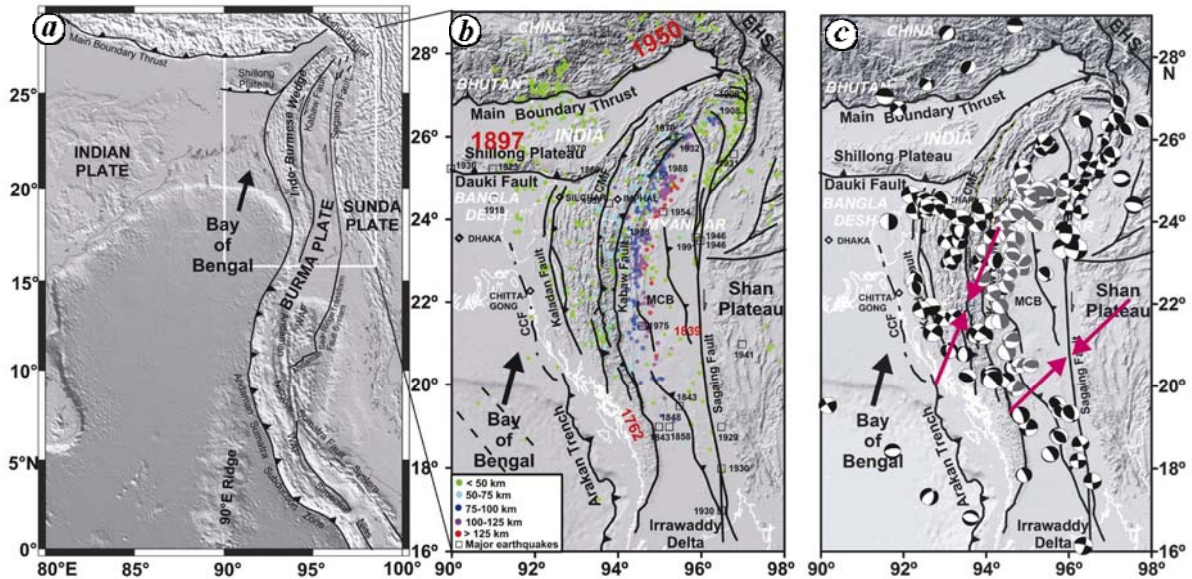
---

**Figure 1.** General tectonics of the Sunda arc. Arrow in (**a**) shows the India–Sunda relative plate motion (36 mm/year). Seismicity and earthquake focal mechanisms are shown in (**b**) and (**c**). All historical great and major earthquakes are also shown. Pink arrows show the direction of maximum principal stress ($\sigma_1$), derived from the inversion of earthquake focal mechanisms[50]. CCF, Chittagong Coastal Fault; MCB, Myanmar Central Basin; CMF, Churachandpur–Mao Fault; EHS, Eastern Himalayan Syntaxis and WAF, West Andaman Fault.

the Indo-Burmese arc (IBA). The IBA is the plate boundary between India and Burma plates, which is probably one of the least studied domains as far as plate motion, crustal deformation and earthquake occurrence processes are concerned. Here the plate boundary, from west to east, consists of the Indo-Burmese wedge (IBW), Myanmar Central Basin (MCB) and Shan Plateau (Figure 1). Geodynamic setting and earthquake occurrence processes are relatively complex in the IBW and adjacent regions. After the collision of the India plate with the Eurasian plate, the Burma plate which consists of the IBW, MCB along with the Andaman–Sumatra arc, rotated clockwise to become predominantly north-south trending[8] (Figure 2). Approximately north-south trending convex westward IBW joins the east-west trending eastern Himalaya in the north (Figure 1). Maurin and Rangin[9] have studied the structures and kinematics of the IBW, which defines the western margin of the Burma plate, a sliver between the India and Sunda plates. Hence, the Burma plate is a sandwiched micro plate between the Indian plate to the west and the Sunda plate to the east. On the western front of the Burma plate, the IBW displays a different grade of metamorphism and rock types of different chronological order across IBW. These different chronological litho units are separated by fossil thrust sheets, namely from west to east transect across IBW region, Chittagong Coastal Fault (CCF), Kaladan Fault (KLF), Churachandpur–Mao Fault (CMF) and Kabaw Fault (KBF) respectively. The Sagaing Fault (SF) marks the eastern boundary of the Burma plate of the northwestern Sunda arc (Figure 1).

Due to the absence of detailed seismo-tectonic studies and geodetic measurements across the IBW, debate con-

tinues about the most appropriate plate boundary model amongst those available, which include active subduction, transform, hyper-oblique and no plate boundary at all[10–15]. Several frontline evidences that include arc magmatism and metamorphism[16,17], occurrence of ophiolitic rock sequence[18], surface as well as subsurface expression of fold and thrust belt-associated structures[11,12,19], gravity anomalies[20], tomographic images[21,22] and palaeo-geographic reconstruction[8,23], confirm that subduction occurred in geological past, but whether it is still active in recent times is a debatable topic. Another question in this context is how the relative plate motion between the India and Sunda plates is accommodated across IBW region – whether it is localized, partitioned or distributed? Recent GPS measurements[5,24] across the Sagaing/Shan Scarp Fault system of Myanmar suggest that SF accommodates about 20 mm/year through right-lateral strike–slip motion of the plate convergence of about 36 mm/yr between India and Sunda plates. Due to lack of sufficient geodetic measurements and their analysis, it is not known where and how the remaining plate motion of about 16 mm/year is accommodated. Our objective is to address the above-mentioned unresolved issues in this article.

## Seismo-tectonic studies

### Current seismicity

The complex geodynamic setting of IBW and adjoining regions makes the earthquake occurrence process in this region enigmatic. Earthquakes in the IBW and SF regions occur in response to the accommodation of the India–Sunda plate motion along these two distinct

boundaries. Under the accretionary wedge, majority of the earthquakes occur in the depth range 30–60 km and define an eastward gently dipping (~ 10°–15°) seismicity trend surface that coincides with the Indian slab (Figure 3). The dip of the slab steepens in the eastern direction and earthquakes occur to a depth of 150 km, though the slab can be traced up to the 660 km discontinuity[21]. Although these features are similar to a subduction zone, the nature of the earthquakes and our recent analysis of their focal mechanisms suggest that these earthquakes are of intra-plate type. They occur on steep planes within the Indian plate, and the nodal planes of these earthquakes are mostly oblique to the strike of IBW. The derived orientation of maximum principal stress ($\sigma_1$) is in the NNE–SSW direction and the sense of motion on the nodal planes implies a northward relative motion with respect to the Sunda plate (Figure 3). Presence of a few intra-plate earthquakes with normal faulting mechanisms in IBW are also generally consistent with the derived maximum principal stress ($\sigma_1$). Some of them represent earthquakes in outer rise. Thus, these earthquakes and the stress state derived from the inversion of the earthquake

focal mechanisms do not support active subduction across IBA, which is also consistent with the predominant northward motion of the India plate with respect to the Sunda plate along this north-south-oriented plate boundary[25] and the GPS measurements presented in the present article. In the SF region, earthquakes occur through right lateral strike–slip motion along the north-south-oriented plane and the stress state is consistent with the plate motion across the SF[25].

*Historical seismicity*

Kundu and Gahalaut[25] compiled a catalogue of major earthquakes in IBA and SF regions (Figure 1)[12,26–29].



**Figure 3.** A depth section across the Indo-Burmese Wedge (IBW) and Sagaing Fault showing the seismicity, earthquake focal mechanisms (east-west vertical cross-sectional projections) and topography. Note the steep nodal planes of the earthquake focal mechanisms which are not consistent with the gentle dip of the seismicity trend under the IBW.
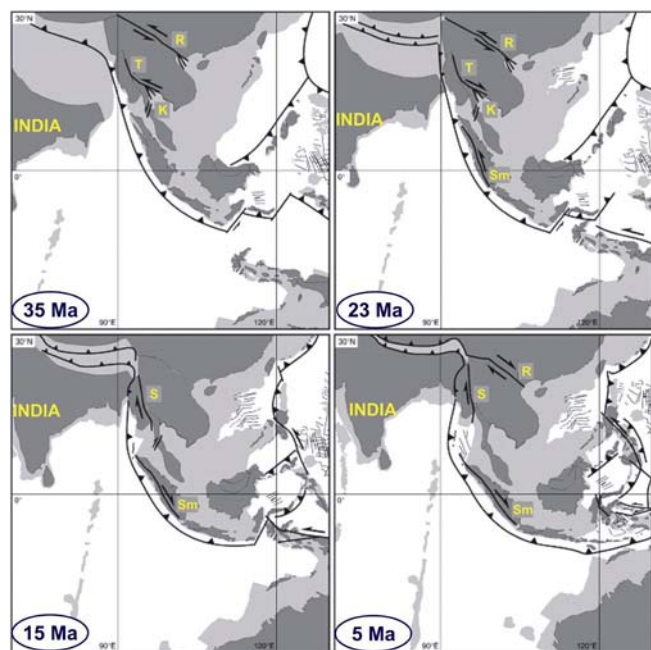


**Figure 2.** Reconstruction of the Sunda land region at 35, 23, 15 and 5 Ma based on Hall[8]. At 35 Ma, India–Asia collision was underway and extrusion of Indo-China began by sinistral movement along the Red River Fault (R) and sinistral movement along the Three Pagodas–Mae Ping Faults (T). There was sinistral movement on the Ranong–Klong Marui Fault (K) system. At 23 Ma, collision with Australia started in East Indonesia and widespread plate reorganization began. The Red River Fault remained sinistral, but movement direction changed to dextral on the Three Pagodas–Mae Ping Faults. Dextral movement on the Sumatra Fault (Sm) began. At 15 Ma, movement on the Red River Fault ceased. Dextral movement on the Sumatra (Sm) and Sagaing (S) Faults was linked via extension in the Andaman Sea. At 5 Ma, there was dextral movement on the Red River Fault, the Sumatra Fault and Sagaing Fault and oceanic spreading was underway in the Andaman Sea.
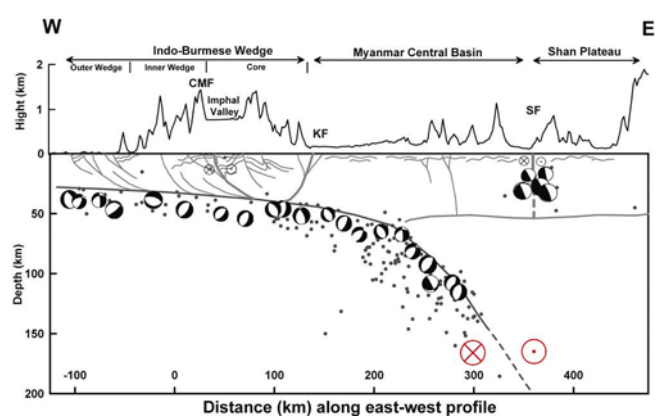


**Figure 4.** (*a*) Historical Govindaji temple and the accompanying structure, the Beithoub, in the Kangla palace, Imphal was damaged during the 1869 Cachar earthquake. Other historical temples in the region did not appear to have suffered any damage from the earthquakes. However a small tilt (~ 4°) was observed at the Madan Mohonji temple (*b* and *c*) which may not necessarily be ascribed to the earthquake.

**Figure 5.** Historical temples in Silchar (South Assam) region. Note extensive ruins of the Khaspur king's ward (*b*) and two temples (*a* and *d*) at Taligram. Due to restoration work at other two temples (*c*, *e* and *f*), damage assessment is not possible. *f*, Singhdwar, note the extensive tilt. The observed tilt in (*a*) and (*f*) appears to be due to local site affects.

We excluded earthquakes occurring in the Shan Plateau and Red River Fault region as they are linked with the tectonics of the Tibet Plateau extrusion due to the India–Eurasia convergence. Although there are a few unverifiable reports of earthquake occurrence as early as 1548 in Tripura, Assam or Bangladesh[27,29], there are large uncertainties in the earthquake location. We find that the catalogue is probably reliable only after 1762.

We studied historical earthquakes by exploring the damage to historical monuments and temples in Silchar, Imphal and adjoining regions of Manipur valley (Figures 4 and 5). The 10 January 1869 Cachar–Manipur earthquake was the most severe earthquake in the available 2000 years of written historical records of Manipur[30,31]. Earlier, Manipur was an independent kingdom[31], which was ruled by Meitei kings since 35 CE. Kangla (now Imphal) in Manipur valley was the capital of the princely state and the historical records were maintained in *The Cheitharol Kumpapa*, *The Court Chronicle of the Kings of Manipur*[30,31]. In these records, occurrence of only the 1869 earthquake which caused damage in the Cachar valley near Silchar and Manipur valley near Imphal, has been mentioned. We visited more than 12 historical temples, the oldest among them being about 400 years. We did not find much evidence of damage in the Manipur and Cachar valleys due to the 1869 earthquake (Figures 4 and 5). The damage was mainly confined to small pockets, e.g. the Kangla palace in Imphal. At other places the old historical structures did not suffer damage either due to the fact that they were small and massive or the site conditions were better. Lack of evidence of occurrence of great earthquakes in the historical records and absence of

occurrence of inter-plate earthquakes in the IBA demand careful analysis of how the plate motion in this region is accommodated and what is the seismic hazard due to the great earthquakes in IBW.

## GPS measurements of crustal deformation

### Methodology

To quantify plate motion, GPS measurements of crustal deformation in IBW were initiated in 2004 with the establishment of 26 survey-mode and three permanent GPS sites (Figure 6). The survey-mode sites have been occupied annually from 2004 till 2011. Twenty-six campaign-mode GPS sites in IBW were occupied annually for 3–4 days. GPS data from these sites, including 20 IGS sites during 2004–2011 were processed using the GAMIT/GLOBK software, version 10.4 (refs 32–34). The station coordinates and their rates are estimated in the ITRF-2005 reference frame. These data were processed on a daily basis producing loosely constrained station coordinates and satellite orbits. These were further combined with loosely constrained solutions of globally distributed nearby IGS station data available from the Scripps Orbital and Positioning Analysis Centre (SOPAC; http://garner.ucsd.edu). Using the GLOBK software, position estimates and velocity stabilization in ITRF-2005 were achieved. The coseismic and post-seismic displacements due to the 2004 Sumatra–Andaman earthquake (*M* 9.2) are negligible[24] and hence ignored. We have represented the velocities in the India fixed reference frame using the Euler rotation pole of the stable Indian plate,

proposed by Banerjee et al.[35]. Further, in order to represent the entire plate circuit, we have combined our well-constrained GPS measurements with result obtained from the Myanmar region[5]. The result obtained from Myanmar network has been derived from only two campaigns (1998 and 2000 respectively) and hence may not be accurate, specially for those sites which are isolated. Hence, motion from these isolated sites is ignored. In order to bring similarity in the reference frame representation, transformation from ITRF-2000 to ITRF-2005 is applied using velocity field comparison and combination version 1.01 (VELROT) for the data incorporated from the Myanmar network[5].

*Observations*

The following observations can be made from the GPS measurements in the region (Figure 7).

(1) Estimated velocity at all these sites in ITRF-2005 is in the NE direction, which varies in magnitude from 45 to 55 mm/year. Slower velocity is observed at sites in the eastern Manipur and eastern Nagaland regions.

(2) The estimated motion at these GPS sites with India fixed reference frame increases in the eastern direction and is predominantly in the SW direction (Figure 7). There appears to be sudden change in the magnitude of the motion near the longitude 93–93.5°E, which corresponds to a known fault, CMF. In the

Imphal valley region, it marks the western margin of the valley itself. One of the immediate interpretations from these observations is that the CMF is a dextral strike–slip fault. It is probably one of the older thrust sheets of this fold-and-thrust belt which is now possibly reactivated in the dextral strike–slip motion.

(3) It is observed that the motion at other GPS sites, e.g. at Kolkata and Bhubaneswar, which should represent the Indian plate motion, is almost similar to that at the westernmost site at MAMT, from where the site motion increases gradually and there appears to be jump at CMF. Thus the CMF may be considered as a plate boundary fault between India and Burma plates.

(4) GPS measurements[5] in the Myanmar region clearly suggest that the Sagaing/Shan Scrap Fault system absorbs about ~ 20 mm/year through dextral strike–slip motion out of the 36 mm/year India–Sunda relative plate motion.

(5) A prominent fault, referred to as the Kopili Fault is located between the Shillong Plateau and Mikir hills, the two main topography features of the region. The approximately northwest-southeast-oriented lineament is considered to be seismically active and extends up to the Himalaya in the north[36]. The two GPS sites, GWHT and TZPR, separated by a distance not more than 120 km, are located on the either side of this fault (Figure 7). The two sites on either side of the Kopili Fault show differential motion of about $2.9 \pm 1.5$ mm/year and imply dextral motion on the northwest-southeast trending fault which is consistent with the available focal mechanism of earthquakes from the region[36].

(6) We did not find any significant motion across KLF and KBF, the two most prominent faults in IBW (Figure 7).

*Preliminary conclusions*

The velocity estimates in ITRF-2005 suggest that the eastern block moves slower than the western block. It becomes clearer in the velocity estimates with reference to the Indian plate. The sites in the western block move slower, as if they are located on the Indian plate. Ideally speaking, the velocity of the westernmost sites (i.e. MAMT, KASH, etc.) should be zero in India fixed reference frame. Such residual velocity at these sites may be explained, either due to error in estimation of the Euler pole for Indian plate which was used to theoretically predict the velocity at these sites, or due to influence of motion of sites on the eastern block due to contribution from the not so perfect elastic/rigid motion.

Sites in the eastern block show significant south to southwestward motion with respect to the Indian plate.
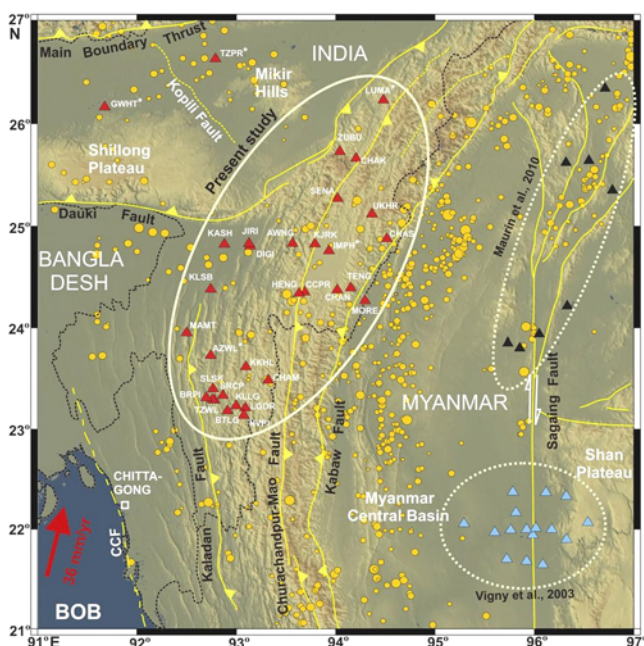


**Figure 6.** GPS networks in the IBW and Sagaing Fault region[5,24]. Filled circles represent the earthquakes in the region. Permanent sites are marked by an asterisk. CCF, Chittagong Coastal Fault.
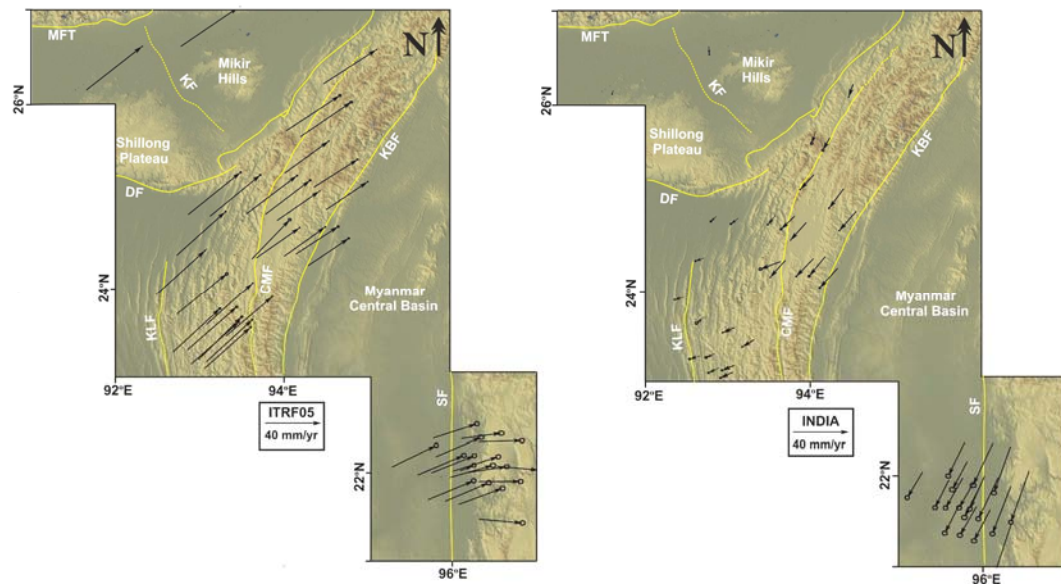
**Figure 7.** Velocity of sites in the IBW and Sagaing Fault[4] region in ITRF2005 (left panel) and Indian reference frame (right panel). MFT, Main Frontal Thrust; SF, Sagaing Fault; KF, Kopili Fault; KLF, Kaladan Fault; CMF, Churachandpur–Mao Fault; KBF, Kabaw Fault; DF, Dauki Fault.

This is the motion which was expected from this region. We further recall that with respect to the Sunda plate, the Indian plate moves northward at a velocity of 36 mm/year, out of which about ~ 20 mm/year is accommodated across SF in the east; hence the remaining motion of about 16 mm/year should be accommodated in IBW through dextral motion. With respect to the Indian plate, this motion will be towards south to south-southwest. Since the motion is almost parallel to the mapped faults in the region, it may be suggested that motion occurs predominantly through dextral strike-slip manner and no or very little dip–slip motion occurs in the region. It supports the hypothesis that there is no subduction across this margin.

Now it is time to pose the big question, 'Where and how is this motion occurring?' Looking at the velocity plots (Figure 7), the two blocks in IBW appear to be distinctly demarcated by the CMF. It appears to be equivalent of the Lelon Fault mapped in Myanmar[9]. The fault can also be well-traced in the satellite imageries (A. K. Saraf and J. D. Das, unpublished[37]). We have further explored the location and characteristics of the CMF through field studies (Figure 8). The SRTM topographic map demarcates a well-defined topographic front west of the Imphal valley in the Manipur region (Figure 8), which is the location of the CMF. In this region there is an east-west trending road, which crosses the north-south-oriented fault zone area, maintained by the Border Road Organization (BRO). However, the stretch of the road in the fault zone is badly damaged, despite several attempts by BRO to repair it. The width of the fault zone is not more than 350–400 m and the deformation appears to be localized in that region. Field investigations further pro-vide us some interesting signatures regarding active nature of the fault zone. Within this stretch of 300–400 m, we identified several landslide zones, tight folds, pulverized material, well-exposed fault gauge and breccia units and associated fault surface (Figure 8). All these evidences suggest that the deformation here is very intense and localized in a narrow zone. Interestingly, not a single major, moderate or small earthquake has been reported from the CMF region either in the global earthquake catalogues or in the available local earthquake catalogue (India Meteorological Department). However, it may be possible to detect relatively lower magnitude events through installation of a local seismic network.

We believe that this fault accommodates the dextral strike–slip motion (as discussed above and shown in Figure 7), which in geological time, acted as the thrust fault. Another point to ponder is whether the motion is seismic or aseismic. The velocity with reference to the Indian plate suggests that the increase in velocity in the eastward direction is sudden, rather being gradual. A gradual increase in velocity will indicate strain accumulation, whereas the sudden increase like a 'jump' will indicate aseismic motion across the boundary. We explore this in subsequent sections.

## Estimation of strain rate from GPS-derived velocity

Fitting a strain model to GPS-derived displacement/velocity data (i.e. inverse strain modelling) is the first-order qualitative interpretation of the data. GPS-derived velocities in India fixed reference frame (Figure 9) clearly show that velocity on either sides of the CMF is
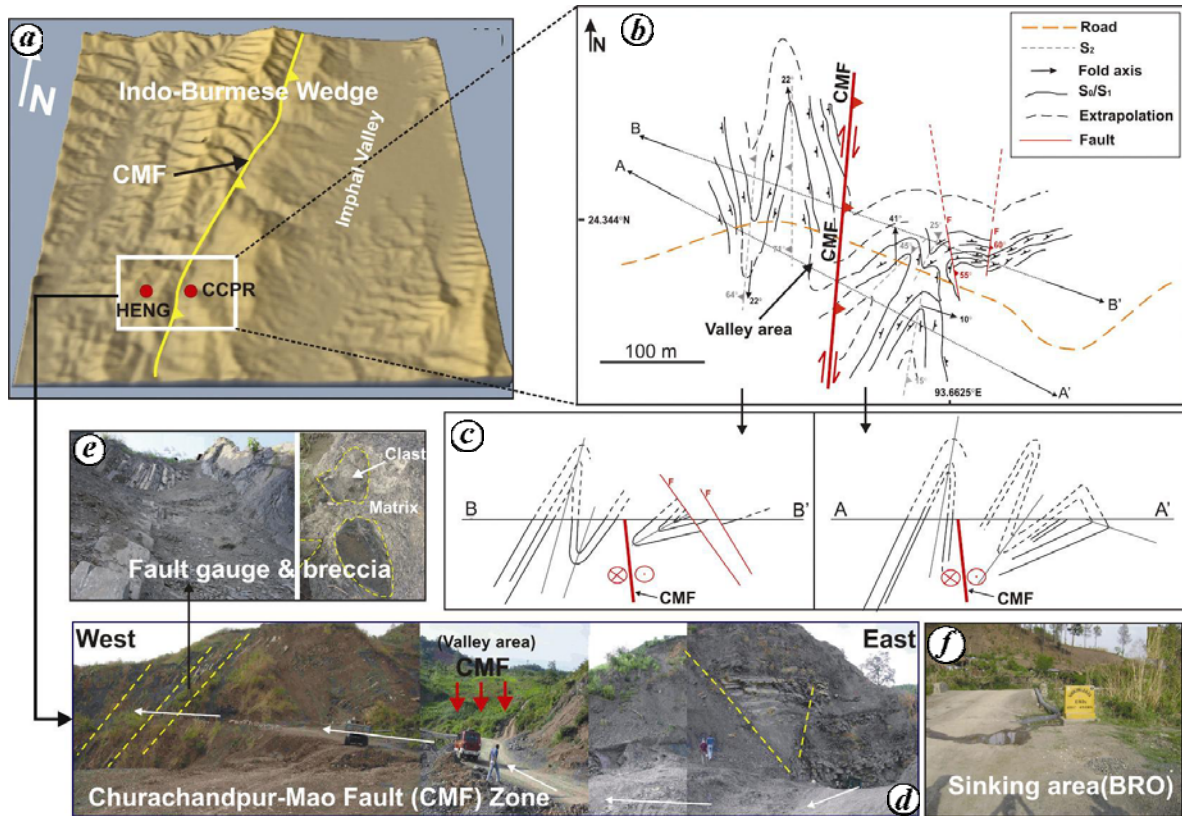
**Figure 8.** Field study in the Churachandpur–Mao Fault (CMF) zone, near Churachandpur. ***a***, Digital Elevation Model of the IBW, showing topographic front marking CMF. The two nearest GPS sites to CMF are also indicated. ***b***, General structural map of the CMF zone. ***c***, Two cross-sections (*A–A′* and *B–B′*) are shown. Location of CMF is the valley area (red bold line) is also shown. ***d***, Composite field photograph of the CMF zone. The winding road is shown by white arrow. The CMF location is marked by red arrow. ***e***, Fault gauge and breccia are shown. The signboard 'sinking area' by the Border Road Organization (BRO) marks the eastern limit of the fault zone.
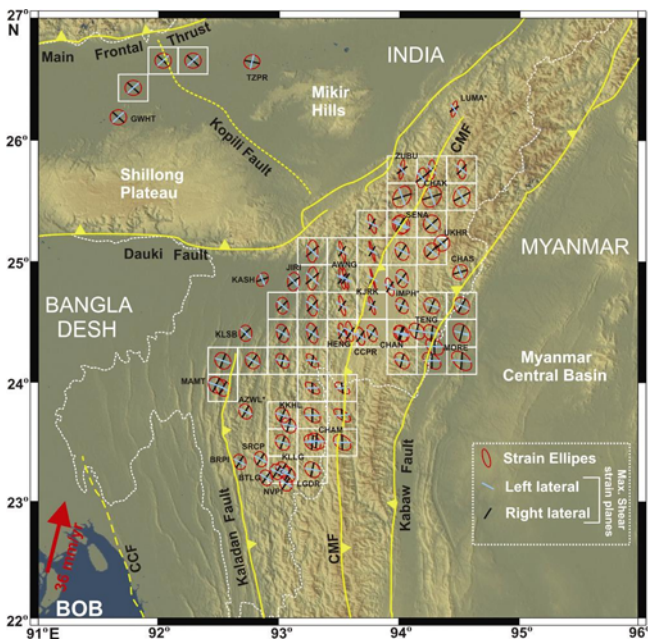


**Figure 9.** Horizontal principal strain rate axes derived from the GPS displacement rate, estimated in a regular grid according to the distance weighted approach. Note the highly deformed strain ellipse near the CMF. BOB, Bay of Bengal.

significantly different. This evidence motivates us to further analyse the strain rate across CMF. We have estimated the horizontal 2D strain rate principal axes and their directions on a specified grid, by weighting data. It is performed using SSPX (a Macintosh, Cocoa/Universal application)[38] computer program, by applying the distance-weighted approach on a regularly spaced grid to estimate the strain using all GPS sites. The advantage of this application is that SSPX works equally well for small deformation (i.e. infinitesimal strain) and for large deformation (i.e. finite strain) associated problems. The data points from each station are weighted by their distance from the grid node, by defining a constant, $\alpha$, which specifies how the effect of a station decays with distance from the node[38,39]. Each datum is weighted by a factor $W$:

$$W = \exp[-(d^2/2\alpha^2)],$$

where $d$ is the distance between the node and a station. Stations within $1\alpha$ distance contribute more than 67% to the least squares solution, whereas those at greater than $3\alpha$ contribute less than 1% (ref. 39). We have used 25 km grid spacing and distance weighted algorithm with $\alpha = 30$ km. The value of $\alpha$ is chosen so that it yields
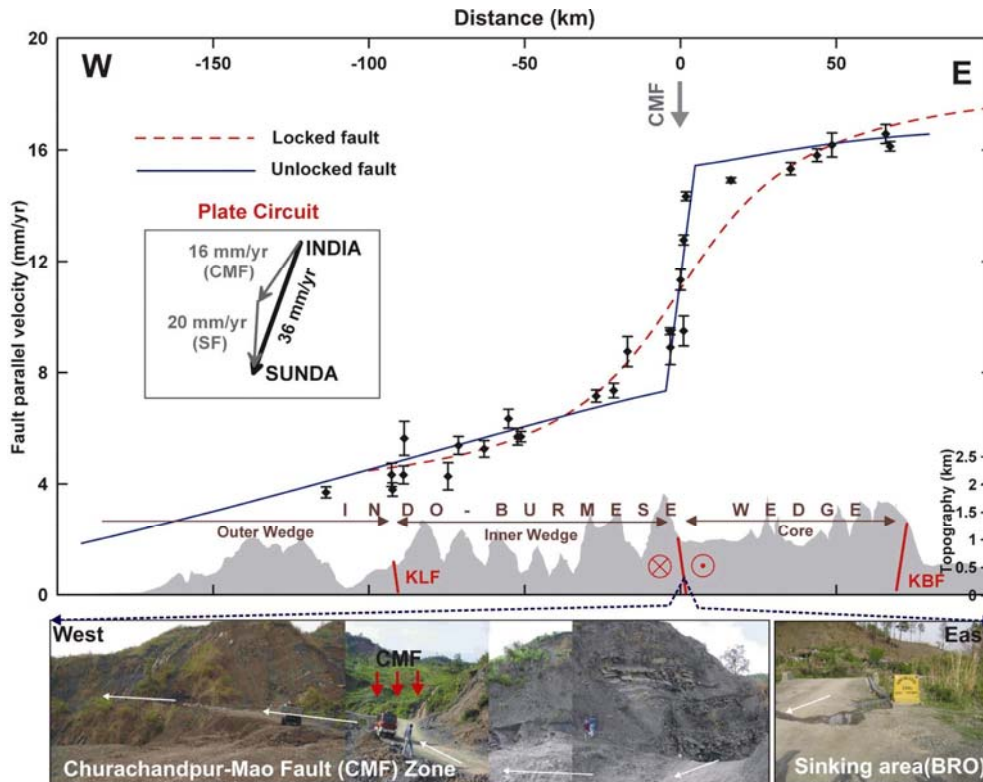
**Figure 10.** A profile perpendicular to the CMF (approximately in the east-west direction) showing fault parallel site velocity. Red dashed curve is the simulated velocity profile (rms misfit ~ 0.15 mm/year) due to locking on CMF at a rate corresponding to the dextral strike–slip motion of 16 ± 2 mm/year. The continuous blue curve (rms misfit ~ 0.08 mm/year) corresponds to the relative motion of 16 mm/year across the IBW, largely accommodated on CMF with very low friction of 0.18. (Inset) Partitioning of the India–Sunda plates, motion on CMF in the IBW and Sagaing Fault (SF).

maximum variation in the parameter of interest with minimum number of insignificant nodes, where the absolute value of the magnitude is less than the $1\sigma$ uncertainty. $W$ is represented as a diagonalized matrix and included in the inversion as[40]

$$a = [M^T W M]^{-1} M^T W b,$$

where $a$, $b$ and $M$ are the unknown model parameter, displacement/velocity and matrix representing initial or final positions of the stations (i.e. the design matrix) respectively.

Figure 9 shows the estimates of stain ellipses, with maximum shear strain rates and rotational strain rates estimated on the rectangular grid. From this strain analyses the following salient features are documented.

(i) Maximum shear stain rate (0.165 μ strain/year with azimuth of ~ 31°) is observed along the CMF (Figure 8). Moreover, the trend of the right lateral shear strain direction also coincides with the general trend of the surface-mapped CMF. However, the maximum value of extension rate and shortening rate is less compared to the maximum shear strain rate. Thus the

GPS-derived stain rate suggests that the CMF actually accommodates a considerable amount of relative motion in IBW through dextral motion.

(ii) GPS-derived strain rate and the general trend of the right lateral shear plane are consistent with the general trend of the Kopili Fault (Figure 9).

## Modelling of GPS data

We resolved the Indian reference frame velocity estimates into the CMF parallel and CMF normal components. We find that there is no significant variation in the fault perpendicular motion across the CMF, implying that there is no subduction across the CMF or any other fault in the IBW. However, significant increase in the fault parallel velocity from west to east implies that the slip along the CMF is accommodated through dextral strike–slip manner, either through stick and slip behaviour or through aseismic creep (Figure 10). We assumed the steeply dipping CMF to be locked and the plate boundary interface further downdip to be slipping freely. Although the simulated strain accumulation curve[41] corresponding to a downdip fault width of 25 km and a dextral slip deficit rate of 16 mm/year on a very steep fault with dip as

80° simulates the overall pattern in the fault parallel velocity, it fails to simulate the sudden jump at CMF (Figure 10). These estimates were derived using the grid search method.

The sudden jump in the velocity may actually imply that the deformation across CMF may be due to aseismic slip involving very low friction. To test this, we used a finite element method (ANSYS software) in which friction may vary on the CMF. ANSYS employs the Newton–Raphson approach to solve nonlinear problems. In this method a load is subdivided into a series of increments applied over several steps. Before each solution the Newton–Raphson method evaluates the out-of-balance load vector, which is the difference between the restoring forces and the loads corresponding to the element stresses and the applied loads.

In our model, the CMF is considered as a steeply dipping fault, which joins the plate boundary interface between the Indian plate and Burma sliver (Figure 11). We considered a two-layer model in which the upper layer represents IBW, whereas the lower layer represents the Indian plate. The material in both the layers was considered to be perfectly elastic. On the basis of the seismicity data[25] and seismological studies related to receiver function[42], the wedge thickness was considered as 25 km. The friction on the CMF in the wedge (in the upper layer) was allowed to vary, while on the plate boundary interface in layer 2, it was assumed as zero (actually it was considered as 0.05, to avoid singularity) to simulate the steady aseismic slip. The entire model covers a tetrahedron prism with horizontal dimensions of 375 km (along the east-west direction) × 200 km (along north-south direction) and a depth extent of 45 km. The model is composed entirely of four-node tetrahedron solid structural elements, and consists of 54,039 elements with 11,214 active nodes. The mesh was refined at the frictional contact surface and consists of 1106 active nodes at the surface. All elements deform elastically and follow Coulomb friction failure criterion. The force for the Coulomb friction is

$$
F_f = \begin{cases} K \cdot u_t : \ K \cdot u_t \leq \mu \cdot F_n \ \text{(sticking)}, \\ \mu \cdot F_n : \ K \cdot u_t > \mu \cdot F_n \ \text{(sliding)}, \end{cases}
$$

where $u_t$ is the tangential displacements, $\mu$ the friction coefficient and $K$ is the stiffness coefficient.

The model is subjected to gravity, which compressed the model and established an initial stress state. The bottom of the model was constrained to zero displacement in the vertical direction, and the model sides were not permitted to move vertically (fixed in $Y$ direction). All other nodes were given two DOF, i.e. in $X$ and $Z$ directions. Thus, the velocity of the western part (i.e. representing the Indian plate) of the model is fixed to zero. We imposed a velocity of 18.6 mm/year towards 222°N on the eastern edge of the model which corresponds to the site velocity at MORE, the easternmost site of our network located at the eastern margin of the wedge. The free surface is fully deformable. All velocity constraints are imposed on the model edges as described above and no constraints are imposed on elements within the model. Pore fluid pressure was assumed to be hydrostatic. Results were considered along an east-west profile on the surface passing through the centre.

We find that the resulting velocity estimates across the wedge using a friction coefficient of 0.18 on the CMF provides better fit in the data and simulates the velocity jump reasonably well (Figure 11). The boundary conditions, e.g. dimension of the model, depth of the top surface of the Indian plate, geometry of the fault and far-field applied displacement at the eastern and western margins of the model, have been constrained from various data and observations. The result of low friction is quite robust and does not vary with slight change (e.g. 10%) in these boundary conditions. The very low friction coefficient and the jump in the fault parallel velocity imply aseismic slip on the CMF. Low frictional behaviour on the CMF appears to be related to the fault gauge. From the above, we summarize that out of the 36 mm/year of India–Sunda plate motion, $16 \pm 2$ mm/year (about 43%) is accommodated through dextral motion along the CMF in the IBW and $20 \pm 3$ mm/year (about 57%) is accommodated along SF[5,24] (Figure 10). However, the motion across the CMF is aseismic, whereas it is through stick and slip behaviour across SF.

## Discussion

GPS measurements in IBA have led to some major advancements in understanding the geodynamic complexity of region, viz. in assessing seismic hazard in the region and understanding long-term plate motion across this
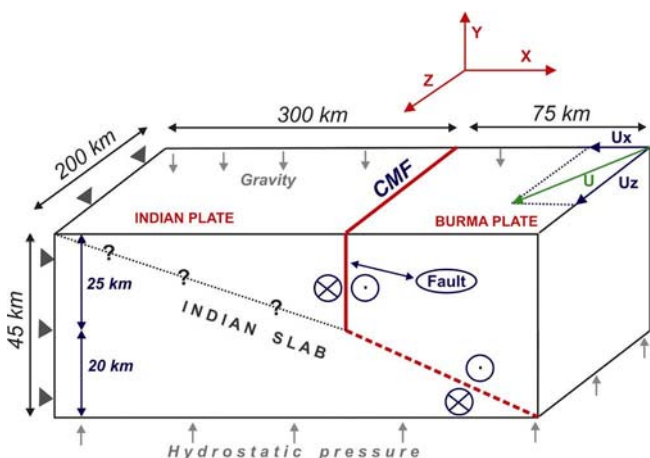


**Figure 11.** A generalized model of the simulation. *U* corresponds to the site velocity of the easternmost GPS site, MORE.
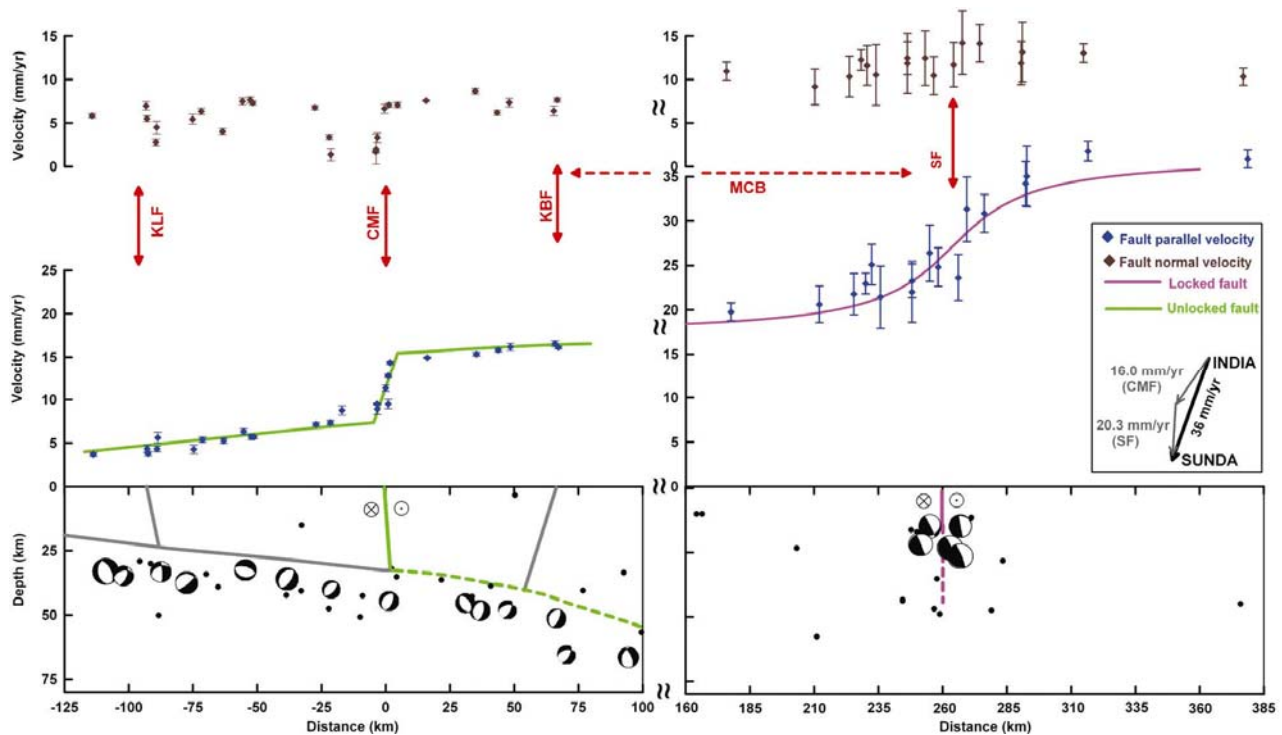
**Figure 12.** Fault parallel and fault normal motion along east–west profile in the IBW and Sagaing Fault (SF) region. There is no apparent jump in the fault normal velocities across the two tectonic features, implying that there is no subduction along this margin. The jump in fault parallel velocity in the IBW and SF region is simulated with aseismic slip of $16 \pm 2$ mm/year along CMF and seismogenic slip of $20.3 \pm 3$ mm/year along SF[5,24]. (Inset) Partition of the India–Sunda plate motion along CMF in IBW and SF. Lower panel shows the geometry of the faults. Dashed portion of the fault at depth (or plate boundary interface) denotes stable sliding. KLF, Kaladan Fault; KBF, Kabaw Fault; MCB, Myanmar Central Basin.

hitherto complex plate boundary region which had no or limited geodetic data.

### Implication of aseismically slipping boundary: seismic hazard assessment

From the available historical records of the past several years, it appears that no great earthquake has occurred in the IBA region, or more specifically on the CMF. The great 1897 Shillong Plateau and 1950 Assam earthquake occurred in the Shillong Plateau and Himalayan region respectively. Therefore, they are not linked with the tectonics of the IBA region. In the history of more than 500 years, only two strong earthquakes appeared in the IBA region, the 1869 Cachar earthquake and the 1762 Arakan earthquake. However, a careful study of the damages caused by the 1869 earthquake suggests that this was not a great or even major earthquake as the damage due to this earthquake was confined in a small regions where unconsolidated sediments were present (see the earlier section). On the other hand, Cummins[43] reported the 1762 Arakan earthquake as a great tsunamigenic earthquake. The effects of the earthquakes were mostly found to be highly exaggerated[44]. It is now considered that this earthquake probably did not cause any major tsunami[44] and was probably only a major earthquake[45].

Modern seismological history of the past 50 years indicates that the earthquakes in IBW occur at depths greater than 40 km on steep fault planes within the subducted Indian plate and are thus considered as intra-plate earthquakes. Even the largest 1988 Indo-Myanmar border earthquake ($M$ 7.1), occurred at 90–100 km depth regime. The contact surface between the basement of the outer IBW and the Indian plate is non-seismogenic. The CMF, which accommodates a large part of the India–Sunda plate motion, is not associated with any earthquake and slips aseismically and joins the contact surface between the Indian plate and the IBW. Slip on the deeper parts of the contact surface occurs through stable sliding. Thus the motion between the India and Sunda plates is accommodated in the IBA through slip on the CMF occurring aseismically and does not contribute to the strain accumulation. It implies that the earthquake hazard in the IBA region due to great and major inter-plate earthquakes is extremely low. However, we acknowledge this fact that strong intra-plate earthquakes that generally occur at depths greater than 50 km, may cause damage in the sediment-filled valley regions, such as the Cachar and Imphal valley in the Indian and Sylhet trough and Chittagong in Bangladesh, where sediments are unconsolidated.

In the seismic hazard zonation map of India, the entire NE Indian region has been classified in seismic zone V,

the highest seismic hazard zone. This is primarily due to the fact that the great 1897 Shillong Plateau and 1950 Assam earthquakes occurred in the region. We are of the opinion that it is correct to classify the Shillong Plateau region and the Arunachal Himalaya region in seismic zone V. However, in view of our studies, putting the region along IBA (i.e. the states of Nagaland, Manipur, Lower Assam and Mizoram) in seismic zone V, is not appropriate and the proposed high seismic hazard in the region needs to be downgraded.

### Long-term plate circuit between India and Sunda plates

We have combined the results of GPS measurements with those from the SF region in Myanmar[5]. The results of crustal deformation from the central and northern part of the SF region have been derived from only two survey-mode GPS measurements. However, since several sites

have been occupied in the region, the estimate of slip rate of about $20.3 \pm 3$ mm/year across SF may be considered reliable. Thus, out of the India–Sunda plate motion of about 36 mm/year, $20.3 \pm 3$ mm/year (i.e. about 57%) is accommodated through dextral motion on SF (Figure 12), which is currently locked. We propose that the remaining motion at about $16 \pm 2$ mm/year (i.e. 43%) is accommodated through dextral motion along the CMF in an aseismic manner (Figure 12). It also implies that the CMF is the present active plate boundary fault or deformation front.

It has been suggested that in the Sumatra region, the motion between the India and Sunda plates is partitioned between the arc normal motion in the frontal arc and arc parallel motion in the back arc, i.e. on the Sumatra Fault system[12,46]. In the Andaman–Nicobar region the motion in the frontal arc becomes oblique. The motion in the back arc is accommodated through strike–slip and normal motion on the Andaman Sea transform rift system, which joins with SF in the north. It has been suggested that there is no segmentation between FBW in the north and
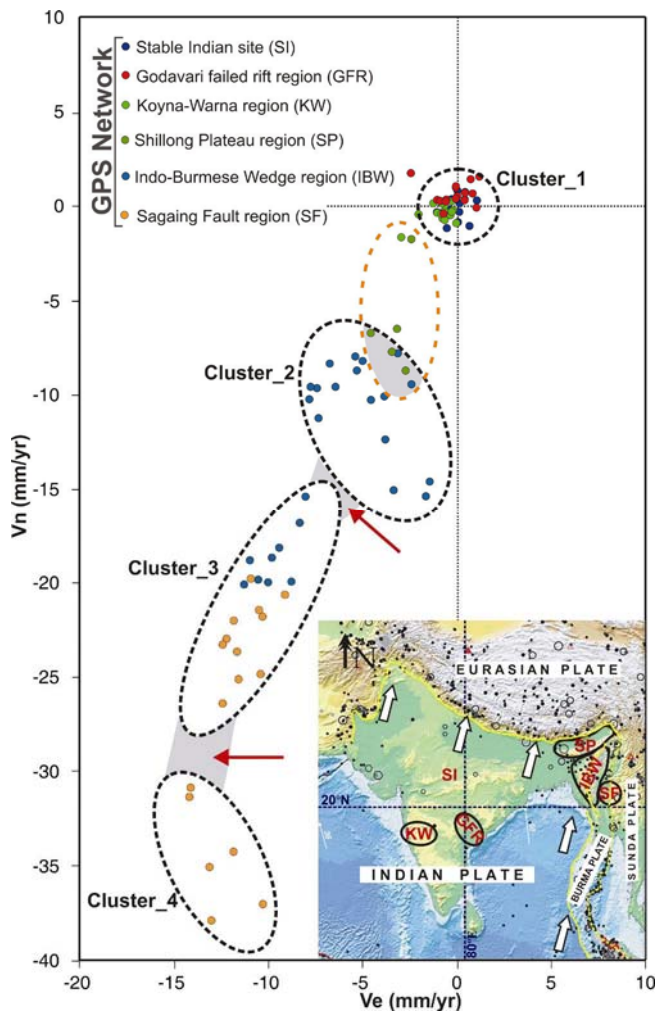


**Figure 13.** Cluster analysis of GPS-derived regional velocity. Four different clusters are identified irrespective of regional networks[2–4] and presence of major active fault biasness. Major cluster gaps are highlighted by red arrows.
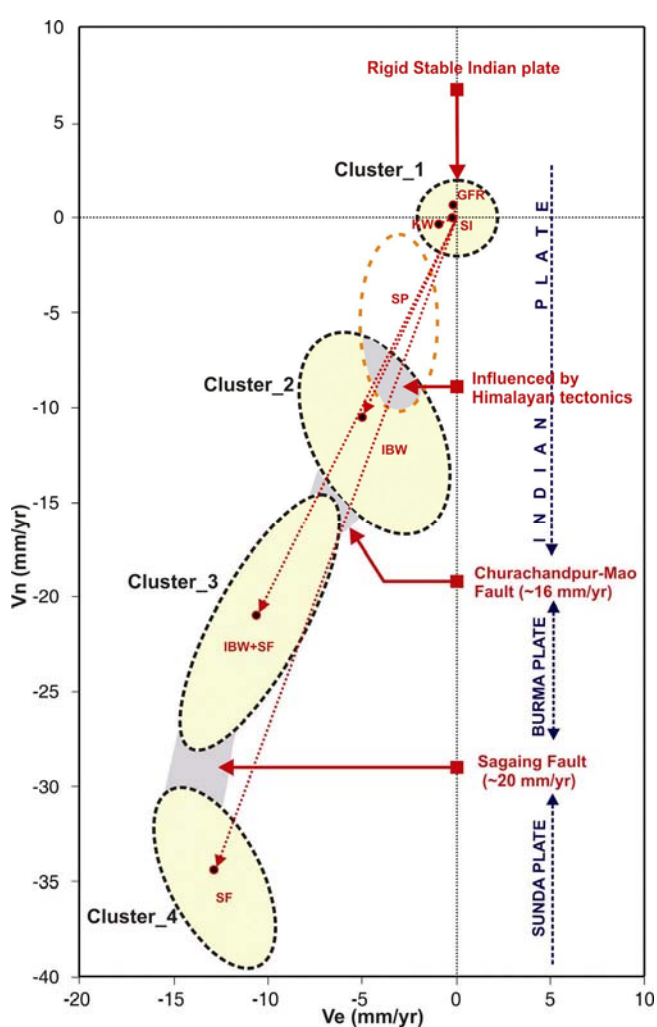


**Figure 14.** Implication of cluster analysis. Note the major active faults are separating the three GPS velocity clusters (i.e. clusters_2–4) of the Indo-Burmese arc (IBA) region.

Andaman–Sumatra subduction zone in the south, as the motion in the two regions can be explained by a single Euler pole[47]. Such an Euler pole predicts predominant strike-slip motion in IBW, which is consistent with the motion derived from GPS measurements. Thus it is appropriate to use term 'partitioning' of the India–Sunda plate motion between the CMF and SF. In this context, it is logical to propose that the deformation front of the India–Burma plate boundary is at the CMF in IBW.

*Subduction to strike–slip transition*

In the context, it is appropriate to analyse the exact nature of the plate boundary in the IBA. We acknowledge this fact that structural transitions from subduction systems to transform faults on oblique or hyper-oblique convergent plate boundaries are often poorly surveyed or overlooked because of lack of direct evidences. However, detailed tectonics studies of such transitions are necessary to identify clearly the modalities of transfer of relative plate motion from transform plate boundary to subduction interface. Approximately 25 such subduction to



**Figure 15.** Schematic illustration showing how applied forces (*F*) and lithospheric rheology ($\mu$, $\eta$) influence GPS velocity field of the Indian subcontinent. The transition from global plate kinematics through continental block models to continuum models is also shown[51]. Hypothetical GPS clusters are shown below. Fcr, Collision resistance; Ftr, Transform resistance; $\mu$, Frictional coefficient for crustal faults; $\eta$, Viscosity of lithosphere; SI, Stable Indian plate; GFR, Godavari Failed Rift region; KW, Koyna–Warna region.

strike–slip transition domains were reported during the 1999 Penrose Conference; for example, both ends of Alpine Fault, New Zealand, northern and southern Carribean, the Scotia Sea, northern California, the western Aleutian, Taiwan, Japan and Kamchatka (http://people.uncw.edu/grindlayn/revabstr_vol.pdf). Here is another example where there is a transition from subduction (in the Andaman–Sumatra region) to the transform plate boundary (in the IBA). However, IBA is anomalous in the sense that here the transition from subduction to strike–slip is not only in space, but also in time. As discussed earlier, there are evidences of subduction and presence of a subducted slab under IBA. But the present GPS measurements and their analysis and the earthquakes in the region clearly suggest that this boundary at present acts as a transform fault boundary.

*Cluster analysis of regional GPS velocity and implication over user-defined model*

Simpson *et al.*[48] suggested that cluster analysis provides a simple visual exploratory tool for the preliminary investigation of regional GPS velocity and an indirect way of representation of long-term plate circuit. It becomes a robust tool for grouping objects with similar properties[49]. This kind of analysis is widely used in many disciplines, including taxonomy and genomics. Simpson *et al.*[48] however, discussed it probably for the first time in the field of 'tectonic geodesy'.

Following Simpson *et al.*[48], here, we have explored the cluster analysis of regional GPS velocity of IBA region (Figure 13). In order to represent contrasting behaviour between plate interior and plate boundary regions, we have also included GPS velocity from stable Indian plate regions[2–4]. It helps us in identifying potentially deforming blocks, usually guided by the distribution of major identified active faults. Irrespective of the network biasness and knowledge of major identified faults, we observe that regional GPS velocity forms four different clusters (Figure 13). Computed cluster means are shown in Figure 14. All individual clusters are separated by major gaps highlighted by red arrows in Figure 13. Note that the velocities defining cluster 1 block in Figure 14, are more tightly clustered than those defining the other blocks (e.g. clusters 2–4). It suggests greater rigidity and lesser amount of internal deformation and elastic strain accumulation within the stable Indian plate. However, GPS velocities belonging to IBA region clearly show greater amount of internal deformation across the major identified active faults (Figures 13 and 14). Interestingly, the Shillong Plateau cluster overlaps with cluster 2 possibly because of the influence of Himalayan tectonics (Figure 14). Our earlier presented plate circuit representation between India and Sunda plates is consistent with this analysis as well (Figure 12). However, the
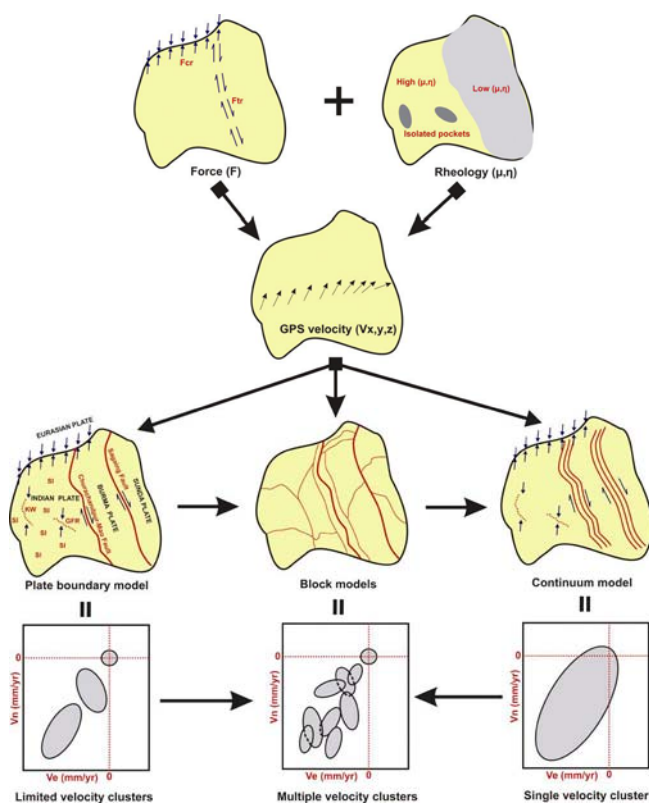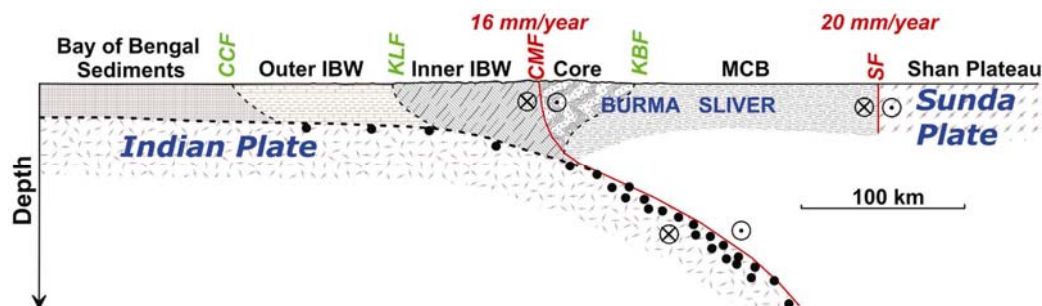
**Figure 16.** An E–W cross-section across IBA and partitioning of plate motion between Indian and Sunda plates. SF, Sagaing Fault; KLF, Kaladan Fault; CMF, Churachandpur–Mao Fault; CCF, Chittagong Coastal Fault, KBF, Kabaw Fault; MCB, Myanmar Central basin.

different user-defined models (e.g. plate boundary, block and continuum models) can be implemented in a slightly different way in the cluster analysis (Figure 15). GPS velocity is a function of two major components, namely force and rheology. Defining models on the basis of observed GPS velocity is dependent on which models we are accepting. The number of GPS velocity clusters will decrease as we approach from 'block model' to 'plate boundary model' to 'continuum model' (Figure 15). We also suggest that there could be locally deforming isolated pockets within the stable Indian plate, e.g. the Godavari Failed Rift region or Koyna–Warna region, that can behave in a slightly different manner. We conclude that GPS measurements provide potential constraints on the spatial distribution of the lithospheric deformation process even in complex tectonic domains.

## Conclusions

Our intensive study, primarily based on GPS measurements, brings the following findings, which resolve some of the geodynamic complexities of the IBA region (Figure 16):

(a) We have found that the CMF, a geologically older thrust fault, accommodates motion of about 16 mm/year through dextral strike–slip manner, which is about 43% of the relative plate motion between the India and Sunda plates. Therefore, CMF is the present-day active deformation front or plate boundary fault between the India and Burma plates.

(b) Most of the evidences, which include lack of historic and great and major earthquakes on the CMF and regions around it, GPS measurements, mathematical modelling with significantly lower value of frictional coefficient, field investigations, etc. favour aseismic behavior of CMF.

(c) Due to the aseismically creeping/slipping active plate boundary in IBW, seismic threat to nearby Manipur, Mizoram, Nagaland, South Assam and adjacent regions, due to large interplate earthquakes on CMF is very low.

(d) Finally, we propose that the IBA region is yet another classical example of subduction to aseismically slipping strike–slip plate boundary transforming tectonic domain in the Indian subcontinent.

1. Faul, H. and Faul, C., In *Began with a Stone*, Wiley, New York, 1983, p. 270.
2. Mahesh, P. *et al.*, Rigid Indian plate: constraints from the GPS measurements. *Gondwana Res.*, 2012, **22**, 1068–1072.
3. Mahesh, P. *et al.*, Localized crustal deformation in the Godavari failed rift, India. *Earth Planet. Sci. Lett.*, 2012, **333–334**, 46–51.
4. Catherine, J. K. *et al.*, Low deformation in the Koyna Warna region, a reservoir triggered earthquake site in west-central India. *Tectonics*, 2013 (in press).
5. Vigny, C. *et al.*, Present-day crustal deformation around Sagaing fault, Myanmar. *J. Geophys. Res. B*, 2003, **108**, 2533; doi: 10.1029/2002JB001999.
6. Pierre, B., Avouac, J.-P., Flouzat, M., Bollinger, L., Ramillien, G., Rajaure, S. and Sapkota, S., Seasonal variations of seismicity and geodetic strain in the Himalaya induced by surface hydrology. *Earth Planet. Sci. Lett.*, 2008, **266**, 332–344.
7. González, P. J. *et al.*, The 2011 Lorca earthquake slip distribution controlled by groundwater crustal unloading. *Nat. Geosci.*, 2012, **5**, 821–825.
8. Hall, R., Cenozoic geological and plate tectonic evolution of SE Asia and the SW Pacific: computer based reconstructions and animations. *J. Asian Earth Sci.*, 2002, **20**, 353–434.
9. Maurin, T. and Rangin, C., Structural and kinematics of the Indo-Burmese wedge: recent and fast growth of the outer wedge. *Tectonics*, 2009, **28**, TC2010; doi: 10.1029/2008TC002276.
10. Sahu, V. K., Gahalaut, V. K., Rajput, S., Chadha, R. K., Laishram, S. and Kumar, A., Crustal deformation in the Indo-Burmese arc region: implications from the Myanmar and Southeast Asia GPS measurements. *Curr. Sci.*, 2006, **12**, 1688–1693.
11. Ni, J. F., Speziale, M. G., Bevis, M., Holt, W. E., Wallace, T. C. and Seager, W. R., Accretionary tectonics of Burma and the three dimensional geometry of the Burma subduction. *Geology*, 1989, **17**, 68–71.
12. Guzman-Speziale, M. and Ni, J. F., Seismicity and active tectonics of the western Sunda Arc. In *The Tectonic Evolution of Asia* (eds Yin, A. and Harrison, T. M.), Cambridge University Press, New York, 1996, pp. 63–84.
13. Nielsen, C., Chamot-Rooke, N., Rangin, C. and the ANDAMAN Cruise Team, From partial to full strain partitioning along the Indo-Burmese hyper-oblique subduction. *Mar. Geol.*, 2004, **209**, 303–327.
14. Satyabala, S. P., Subduction in the Indo-Burma region: is it still active? *Geophys. Res. Lett.*, 1998, **25**, 3189–3192.

15. Satyabala, S., Oblique plate convergence in the Indo-Burma (Myanmar) subduction region. *Pure Appl. Geophys.*, 2003, **160**, 1611–1650.

16. Barley, M. E. *et al.*, Jurassic to Miocene magmatism and metamorphism in the Mogok metamorphic belt and the India-Eurasia collision in Myanmar. *Tectonics*, 2003; doi: 10.1029/2002 TC001398.

17. Bertrand, G. *et al.*, The Singu basalt (Myanmar): new constraints for the amount of recent offset on the Sagaing Fault. *Earth Planet. Sci. Lett.*, 1998, **327**, 479–484.

18. Sengupta, S., Ray, K. K. and Acharyya, S. K., Nature of ophiolite occurrences along the eastern margin of the Indian plate and their tectonic significance. *Geology*, 1990, **18**, 439–442.

19. Pivnik, D. A., Nahm, J., Tucker, R. S., Smith, G. O., Nyein, K., Nyunt, M. and Maung, P. H., Polyphase deformation in a forearc/back-arc basin, Salin subbasin, Myanmar (Burma). *AAPG Bull.*, 1998, **82**, 1837–1856.

20. Mukhopadhyay, M. and Dasgupta, S., Deep structure and tectonics of the burmese arc: constraints from earthquake and gravity data. *Tectonophysics*, 1988, **149**, 299–322.

21. Li, C., van der Hilst, R. D., Meltzer, A. S. and Engdahl, E. R., Subduction of the Indian lithosphere beneath the Tibetan Plateau and Burma. *Earth Planet. Sci. Lett.*, 2008, **274**, 157–168.

22. Pesicek, J. D., Thurber, C. H., Widiyantooro, S., Zhang, H., DeShon, H. R. and Engdahl, E. R., Sharpening the tomographic image of the subducting slab below Sumatra, the Andaman Islands and Burma. *Geophys. J. Int.*, 2010, **182**, 433–453.

23. Bannert, D. and Helmcke, D., The evolution of the Asian Plate in Burma. *Geologische Rundschau*, 1981, 446–458.

24. Maurin, T., Masson, F., Rangin, C., Than Min, U. and Collard, P., First global positioning system results in northern Myanmar: constant and localized slip rate along the Sagaing fault. *Geology*, 2010, **38**, 591–594.

25. Kundu, B. and Gahalaut, V. K., Earthquake occurrence process in the Indo-Burmese wedge and Sagaing fault region. *Tectonophysics*, 2012, **524–525**, 135–146.

26. Chen, W.-P. and Molnar, P., Source parameters of earthquakes and intraplate deformation beneath the Shillong Plateau and northern Indo-Burman Ranges. *J. Geophys. Res.*, 1990, **95**, 12527–12552.

27. Iyengar, R. N., Sharma, S. D. and Siddiqui, J. M., Earthquake history of India in medieval times. *Indian J. Hist. Sci.*, 1999, **34**, 181–237.

28. Ambraseys, N. and Douglas, J. J., Magnitude calibration of North Indian earthquakes. *Geophys. J. Inter.*, 2004, **159**, 165–206; doi: 10.1111/j.1365-246X.2004.02323.x.

29. Steckler, M. S., Akhter, S. H. and Seeber, L., Collision of Ganges–Brahmaputra delta with the Burma arc: implication for earthquake hazard. *Earth Planet. Sci. Lett.*, 2008, **273**, 367–378.

30. Singh, R. K. J., *A Short History of Manipur*, Manipur Sahitya Parishad, Imphal, India, 1965, p. 365.

31. Parratt, S. N., *The Court Chronicle of the Kings of Manipur: 33–1763 CE. The Cheitharol Kumpapa, 1*, Routledge, Taylor and Francis Group, United Kingdom, 1999, p. 305.

32. King, R. W. and Bock, Y., Documentation of the GAMIT GPS analysis software release 10.2. Massachusetts Institute of Technology (MIT), Cambridge, USA, 2005.

33. Herring, T. A., King, R. W. and McClusky, S. C., GAMIT reference manual, Release 10.4. Department of Earth, Atmospheric, and Planetary Sciences, MIT, USA, 2010, p. 171.

34. Herring, T. A., King, R. W. and McClusky, S. C., GLOBK reference manual, global Kalman filter VLBI and GPS analysis program, Release 10.4. Department of Earth, Atmospheric, and Planetary Sciences, MIT, USA, 2010, p. 95.

35. Banerjee, P., Bürgmann, R., Nagarajan, B. and Apel, E., Intraplate deformation of the Indian subcontinent. *Geophys. Res. Lett.*, 2008, **35**, doi: 10.1029/2008GL035468.

36. Kayal, J. R. *et al.*, Large and great earthquakes in the Shillong plateau–Assam valley area of Northeast India Region: Pop-up and transverse tectonics. *Tectonophysics*, 2012, **532–535**, 186–192.

37. Saraf, A. K. and Das, J. D., Earthquake hazard assessment of Indo-Burman tectonic belt based on spatial technologies (RS & GIS), 2010.

38. Cardozo, N. and Allmendinger, R. W., SSPX: a program to compute strain from displacement/velocity data. *Comput. Geosci.*, 2009, **35**, 1343–1357.

39. Shen, Z. K., Jackson, D. D. and Ge, B. X., Crustal deformation across and beyond the Los Angeles basin from geodetic measurements. *J. Geophys. Res.*, 1996, **101**, 27957–27980.

40. Menke, W., *Geophysical Data Analysis: Discrete Inverse Theory*, Academic Press, USA, 1984, p. 260.

41. Okada, Y., Surface deformation due to shear and tensile faults in a half-space. *Bull. Seismol. Soc. Am.*, 1985, **75**, 1135–1154.

42. Mitra, S., Priestley, K., Bhattacharyya, A. and Gaur, V. K., Crustal structure and earthquake focal depths beneath northeastern India and South Tibet. *Geophys. J. Int.*, 2005, **160**, 227–248.

43. Cummins, P. R., The potential for giant tsunamigenic earthquakes in the northern Bay of Bengal. *Nature*, 2007, **449**, 75–78.

44. Gupta, H. and Gahalaut, V., Is the northern Bay of Bengal tsunamigenic? *Bull. Seismol. Soc. Am.*, 2009, **99**, 3496–3501.

45. Martin, S. and Szeliga, W., A catalog of felt intensity data for 570 earthquakes in India from 1636 to 2009. *Bull. Seismol. Soc. Am.*, 2010, **100**, 562–569; doi: 10.1785/0120080328.

46. Curray, J. R., Tectonics and history of the Andaman Sea region. *J. Asian Earth Sci.*, 2005, **25**, 187–232.

47. Gahalaut, V. K. and Gahalaut, K., Burma plate motion. *J. Geophys. Res.*, 2007, **112**, B10402; doi: 10.1029/2007JB004928.

48. Simpson, R. W. *et al.*, Using cluster analysis to organize and explore regional GPS velocities. *Geophys. Res. Lett.*, 2012, 2012GL052755.

49. Kaufman, K. and Rousseeuw, P. J., *Finding Groups in Data, An Introduction to Cluster Analysis*, John Wiley, New York, 1990, p. 342.

50. Michael, A. J., Determination of stress from slip data: faults and folds. *J. Geophys. Res.*, 1984, **89**, 11,517–11,526.

51. Thatcher, W., How the continents deform: the evidence from tectonic geodesy. *Annu. Rev. Earth Planet. Sci.*, 2009, **37**, 237–262.